Hindawi Publishing Corporation
Mathematical Problems in Engineering
Volume 2013, Article ID 530349, 9 pages
http://dx.doi.org/10.1155/2013/530349

Research Article

Performance Recognition for Sulphur Flotation Process Based on Froth Texture Unit Distribution

Mingfang He, Chunhua Yang, Weihua Gui, and Yiqiu Ling

School of Information Science and Engineering, Central South University, Changsha, Hunan 410083, China

Correspondence should be addressed to Chunhua Yang; ychh@csu.edu.cn

Received 30 August 2012; Accepted 20 December 2012

Academic Editor: Bin Jiang

As an important indicator of flotation performance, froth texture is believed to be related to operational condition in sulphur flotation process. A novel fault detection method based on froth texture unit distribution (TUD) is proposed to recognize the fault condition of sulphur flotation in real time. The froth texture unit number is calculated based on texture spectrum, and the probability density function (PDF) of froth texture unit number is defined as texture unit distribution, which can describe the actual textual feature more accurately than the grey level dependence matrix approach. As the type of the froth TUD is unknown, a nonparametric kernel estimation method based on the fixed kernel basis is proposed, which can overcome the difficulty when comparing different TUDs under various conditions is impossible using the traditional varying kernel basis. Through transforming nonparametric description into dynamic kernel weight vectors, a principle component analysis (PCA) model is established to reduce the dimensionality of the vectors. Then a threshold criterion determined by the TQ statistic based on the PCA model is proposed to realize the performance recognition. The industrial application results show that the accurate performance recognition of froth flotation can be achieved by using the proposed method.

1. Introduction

Sulphur flotation is a complex physical process influenced by multiple operational variables such as inlet air flow, pulp level, and it is naturally hydrophobic to attach to the air bubbles. The objective of sulphur flotation is to separate valuable sulphur minerals from useless materials or other minerals so as to gain the upgraded sulphur minerals [1]. Sulphur concentrate grade depends on flotation separation performance, and it is affected by the accuracy of the performance recognition. It is well recognized that froth visual appearance observed can characterize the combining effect of multiple process conditions on flotation [2], and it is also known as the indicator of flotation separation performance. Recent advances in image processing and computer vision based froth appearance monitoring systems contribute greatly to the feature extraction of visual descriptors [3–5]. Computer-based vision technology is now moving out of the research laboratory and into the plant to become a useful means of monitoring and controlling flotation performance at the cell level [6–8]. The development of base level process control (control of pulp level, air flow rate, etc.) has been significant progress, but automated advanced and optimization flotation control strategies based on computer vision have been more difficult to implement [9]. The performance recognition is available for the optimal control of flotation [10], and flotation performance is closely related to the concentrate grade. Therefore, it is of great importance to improve the sulphur concentrate grade by developing an effective performance recognition method based on computer vision.

It is shown that the froth texture is a good indicator to the performance of the flotation cells [11], and texture information is believed to strongly associate with mineral grade [12]. Numerous reported literatures are devoted to the extraction of froth image texture features. The grey-level cooccurrence matrix (GLCM) approach is one of the most popular statistical methods used in practice to measure the textural information of images. Most of the researchers calculated second-order statistics based on GLCM such as angular second moment, entropy, moment of inertia, and moments of deficit and relevance to recognize the flotation performance. GLCM was used as texture descriptor to classify different

types of froths, and they also provide qualitative information on the changes in the visual appearance of the froth [13]. However, there is only one angle of displacement used in the GLCM approach, with 0°, 45°, 90°, and 135° calculated to acquire average second-order statistics, neglecting the different variation in different directions and leading to large computing of the high-dimensional matrix. The actual flotation froth texture is more complex, so that a simple statistical property in the GLCM approach is difficult to accurately describe it, leading to the inaccuracy of performance recognition. Based on the proposed concept of texture unit, a new statistical approach to texture analysis, termed the texture spectrum approach, was proposed [14]. The proposed method extracted the textural information of an image with a more complete respect of texture characteristics (simultaneously in all eight directions instead of only one displacement vector used in the GLCM approach). It is worth noticing that the PDF of texture unit number, defined as the texture unit distribution (TUD), is found to be nonnormal. Further exploring of the information indicated by froth structure has shown that the TUD is multipeaky and highly skewed, which neither belongs to any existing mathematical model based distribution. To depict the unknown continuous process of froth flotation, nonparametric estimation provides a credible solution. Commonly used nonparametric estimation techniques include histogram, frequency polygon, shift average histogram, kernel methods [15], wavelet method, and B-spline expansion models. Theoretical researches on tracking the output probability density distribution to a target distribution shape by using various control approaches [16] can also increase the possibility of froth visual features based process control. Nevertheless, the traditional kernel estimation cannot compare the various froth TUDs under different flotation conditions with the varying kernel basis. Therefore, the fixed kernel basis is proposed to describe the TUDs in various froth images.

To relate the flotation operation condition with flotation performance, Jampana et al. revealed that the increase in pulp level causes concentrate grade to decrease [17], as the variation of pulp level has great effect on the froth retention time in the flotation cell [18]. The continuous decrease of froth retention time can lead to less collision time between mineral particles and bubbles with decreased gangue drop, which resulting in the deteriorating performance of mineral concentrate grade. Conventionally, industry process performance recognition heavily depends on the frequent inspection of froth views and manipulation of experienced human operators, which is often problematic with strong subjective and unable to regulate the fault performance timely, leading to the unstable flotation process and low concentrate grade. Along with the implementation of online monitoring system of froth visual appearance, quantitative performance recognition becomes highly desired and essential to maintain the operational variables at acceptable rates. Cilliers proposed a quantitative fault detection and diagnosis model which is successfully applied for hydrocyclones [19]. In industrial case studies of aluminum flotation, Xu explored the froth structure by using kernel density estimation technique to approximate the output probability density of surface bubble size distribution rectified by the empirical formula and its application on process fault detection [20].

The froth texture characterizes the roughness of the froth surface, which indicates the mineral contents of froth. When the pulp level is too high with slurry overflow, froth texture is smooth; in this case, the middle value takes a large portion of the texture unit number in the whole image, which results in a high peak in the texture unit distribution curve. On the other hand, when the pulp level becomes too low, the froth cannot overflow, such that the mineral contents in the froth accumulate to a high level. Therefore, the texture becomes coarse and the middle value takes a small portion of the texture unit number in the whole image, resulting in a low peak in the texture unit distribution curve. By transforming the texture unit distribution into the weight vector using the fixed kernel estimator, a weight PCA model can be established to handle the variation in the texture unit distribution. The sulphur froth image contains a great deal of noise because of the acid fog in the sulphur flotation. T^2 statistic based on the PCA model can reveal the major variation of the froth texture, and Q statistic can reveal the noise contained in the image. Thus the proposed new statistical variable TQ is proposed to detect the sulphur flotation fault effectively by considering the influence of noise.

The main advantages of the proposed method in this paper are that (i) the texture unit distribution can describe the froth texture feature more completely, by considering eight directions of grey level variation information, compared to the GLCM method. (ii) The mathematical model of texture unit distribution is unknown, as it is nonnormal and multipeaky, so nonparametric estimation method is more suitable to approximate it. The fixed kernel basis can compare the different flotation performance reflected by the weight coefficients of texture unit distribution, compared with the traditional varying kernel basis. (iii) The new statistic TQ can reduce the influence of noise in the accuracy of performance recognition, compared to the traditional T^2 and Q statistics.

This work aims to explore the froth texture by using kernel density estimation technique to approximate the surface froth TUD and its application on sulphur flotation process performance recognition. A nonparametric kernel estimator by the fixed kernel basis is designed to approximate texture unit distribution, such that the output TUD is formulated in terms of dynamic weights, on which a principle component analysis (PCA) model is established. Then an effective performance recognition criterion is determined using the proposed TQ statistic based on PCA model. The fault condition is successfully detected on the industrial data of offline froth images. Next section introduces the froth texture unit number calculation oriented texture spectrum scheme. Section 3 presents the output TUD curve modeling by using designed kernel density estimators. The kernel weight vector based PCA model is established, and a threshold criterion determined by the TQ statistic based on the PCA model is proposed to realize the performance recognition in Section 4. Section 5 presents the experimental results and discussion. Conclusion is provided in the last section.

2. Surface Froth Texture Unit Number Calculation

Experimental setup consists of RGB camera with resolution of 1280×960 and lens of 35 mm, high frequency light source, cover hook protecting camera from dust, acid fog and ambient light, and optical fiber with length over 200 m for signal communication to industrial PC computer in operating room. The camera is mounted 96.5 cm vertically above the froth surface of the target cell, and froth images with window size $24.26 \times 18.2\,\text{cm}^2$ are captured online at the rate of 15 frames/s. Meanwhile, the corresponding process operational and performance data are collected on industrial scale.

Froth images collected from industry field display that various froth texture feature leads to the different performance. The existing texture description method such as texture spectrum, spatial and neighboring grey-level cooccurrence matrix are derived from this fact. Froth image observed is a type of gradient images. Nevertheless, simple second-order statistical variables in the GLCM approach are difficult to accurately describe the froth texture, the texture unit (TU) oriented texture spectrum scheme proposed by [14] is used to describe the texture features. In a froth digital image, each pixel is surrounded by eight neighboring pixels. The local texture information for a pixel can be extracted from a neighborhood of 3×3 pixels called texture unit, which represents the smallest complete unit (in the sense of having eight directions surrounding the pixel). Given a neighborhood of 3×3 pixels (which will be denoted by a set containing nine elements: $V = \{V_0, V_1, \ldots, V_8\}$, where V_0 represents the intensity value of the central pixel, and V_i $\{i = 1, 2, \ldots, 8\}$ is the intensity value of the neighboring pixel i) defines the corresponding texture unit by a set containing eight elements, $\text{TU} = \{E_1, E_2, \ldots, E_8\}$, where E_i $\{i = 1, 2, \ldots, 8\}$ is determined by the following formula:

$$E_i = \begin{cases} 0 & \text{if } V_i < V_0, \\ 1 & \text{if } V_i = V_0, \\ 2 & \text{if } V_i > V_0, \end{cases} \tag{1}$$

for $i = 1, 2, \ldots, 8$, and the element E_i occupies the same position as the pixel i.

As each element of TU has one of three possible values, the combination of all eight elements results in $3^8 = 6561$ possible texture units in total. There is no unique way to label and order the 6561 texture units. In our study, the 6561 texture units are labeled by using the following formula:

$$N_{\text{TU}} = \sum_{i=1}^{8} E_i \bullet 3^{i-1}, \tag{2}$$

where N_{TU} represents the texture unit number, and E_i is the ith element of texture unit set $\text{TU} = \{E_1, E_2, \ldots, E_8\}$.

In addition, the eight elements may be ordered differently. If the eight elements are ordered clockwise as shown in Figure 1, the first element may take eight possible positions from the top left (a) to the middle left (h), and then the 6561 texture units can be labeled by the above formula under eight different ordering ways (from a to h).

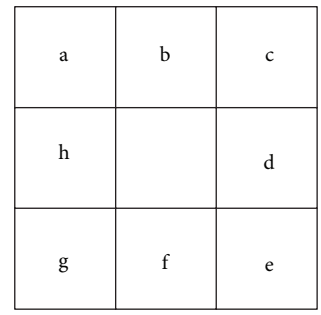

Figure 1: Eight clockwise, successive ordering ways of the eight elements of the texture unit. The first element E_1 may take eight possible positions from a to h.

Figure 2 gives an example of transforming a neighborhood in sulphur flotation froth image to a texture unit with the texture unit number under the ordering way a.

TUD is defined as the occurrence frequency for every texture unit number, and it exhibits probability density function (PDF) distribution of froth texture unit number. The online acquired sulphur froth image in cleaner cell in normal condition is shown in Figure 3. Figure 4 shows the froth TUD. The froth texture unit probability density distribution is found to be nonnormal and multipeaky.

3. TUD Curve Modeling

The surface sulphur froth TUD is nonnormal. Unlike traditional method applying singular feature such as mean or variance with the assumption that the distribution is normal, probability density distribution is suggested to accurately describe statistical feature of froth texture. The fact that the mathematical model of TUD is unknown makes nonparametric estimation method fitting to depict the unknown continuous process of froth flotation.

3.1. Nonparametric Kernel Estimation. Consider a probability density function $f(x)$ describing the probability distribution of x in (a, b) as follows:

$$P(a < x < b) = \int_a^b f(x)\,dx. \tag{3}$$

Density estimation accomplishes the fitting of $f(x)$. Though classic nonparametric histogram estimator is good for data presentation, its discontinuity causes difficulty if derivatives of the estimates are required. A continuous version of the histogram is the frequency polygon formed by interpolating the midpoints of a histogram. Histogram based methods seek the balance between estimation accuracy and feature dimensionality, which can be very expensive for large samples. Apart from the histogram, the kernel estimator is most commonly used [15], which is given by

$$\widehat{f}_{\text{ker}}(x) = \frac{1}{nh}\sum_{i=1}^{n} K\left(\frac{x - X_i}{h}\right) = \sum_{i=1}^{n} w_i K\left(\frac{x - X_i}{h}\right), \tag{4}$$

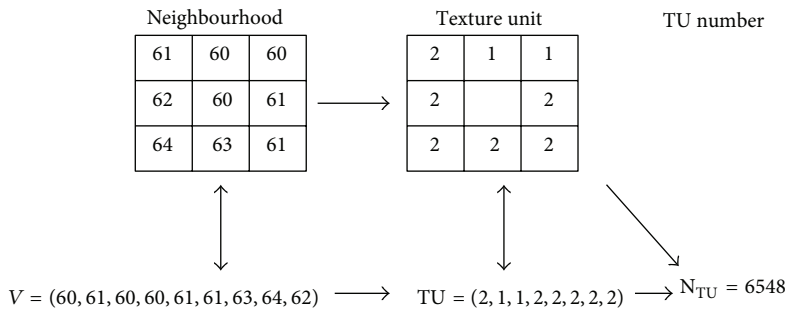

Figure 2: Example of transforming a neighborhood to a texture unit with the texture unit number.

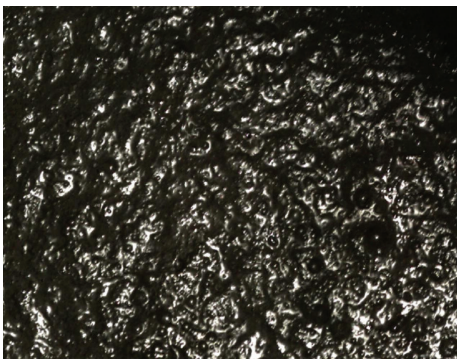

Figure 3: The online acquired sulphur froth images in cleaner cell.

where the function $K(x)$ is the prespecified kernel function satisfying $\int K(x)dt = 1$ to ensure a bona fide density estimate. w_i is the corresponding weight of the ith kernel function, and h is the window width. Based on the prototype of traditional normal kernel function, a kernel function fitting for froth flotation is constructed as

$$K\left(\frac{x - X_i}{h}\right) = \frac{1}{h\sqrt{2\pi}} \exp\left(\frac{-\left((x - X_i)/h\right)^2}{2}\right) \quad -\infty < \frac{x - X_i}{h} < \infty, \tag{5}$$

where $K((x - X_i)/h)$ is the ith kernel function, and X_i is the center of the ith kernel function along the horizontal axis.

3.2. Output TUD Kernel Estimation. Supposing there is a dynamic stochastic system with input $u(t) \in R^m$ and output $y(t) \in [a, b]$, the probability of output $y(t)$ lying in $[a, \xi)$ is defined as

$$P\left(a \le y\left(t\right) < \xi\right) = \int_a^{\xi} f_{\ker}\left(z, u\right) dz, \tag{6}$$

where the $f_{\ker}(z, u)$ represents the output TUD after froth texture unit number calculation. $u(t)$ is control input such as the input amount of pulp level which is a dominant operational condition in the sulphur flotation system. The $f_{\ker}(z, u)$ can be approximated by kernel estimators designed in formula (5) and the corresponding weights w_i.

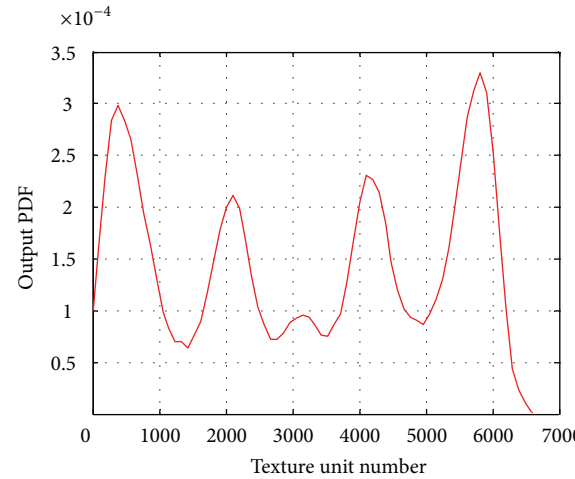

Figure 4: Surface froth texture unit distribution.

Denote

$$K_0\left(z\right) = \left[k_1\left(z\right), k_2\left(z\right), \ldots, k_{n-1}\left(z\right)\right]^T$$
$$W\left(t\right) = \left[w_1\left(u\right), w_2\left(u\right), \ldots, w_{n-1}\left(u\right)\right]^T. \tag{7}$$

Since $\int_a^b \widehat{f}_{\ker}(z, u)dz = 1$, $\int_a^b k_i(z)dz = 1$, $i = 1, 2, \ldots, n - 1$, it is certain that there are $n - 1$ independent weights. So the TUD model is adopted as follows:

$$\widehat{f}_{\ker}\left(z, u\right) = K^T\left(z\right) W\left(t\right) + g\left(W\left(t\right)\right) k_n\left(z\right), \tag{8}$$

where $K(z) = K_0(z)$, $g(W(t)) = 1 - \sum_{i=1}^{n-1} w_i(u)$, $g(W(t))$ is the corresponding weight of $k_n(z)$.

However, the traditional kernel estimation cannot compare the various froth TUDs under different flotation conditions with the varying kernel basis. Therefore, the fixed kernel basis is proposed to describe the TUDs in various froth images, such that the TUD curves can be transformed into dynamic kernel weight vectors, based on which the fault condition can be detected in sulphur flotation. Meanwhile, the computational complexity is also reduced using the designed fixed kernel basis.

Adjusting to the range of froth texture unit number, a number of kernel bases are selected to depict the TUD

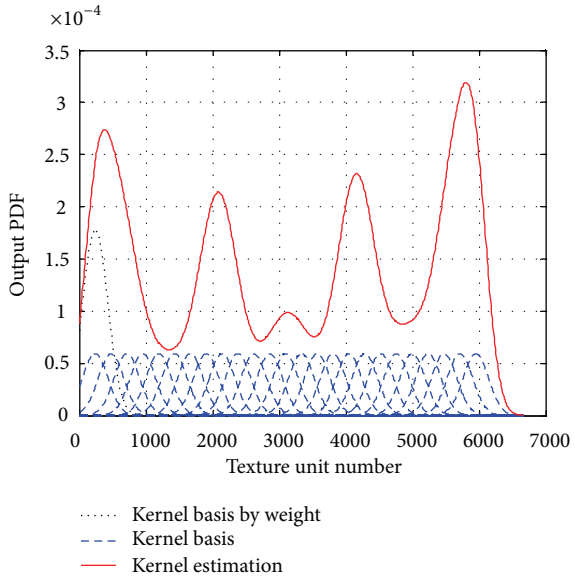

Figure 5: Normal kernel estimation and the weight coefficients.

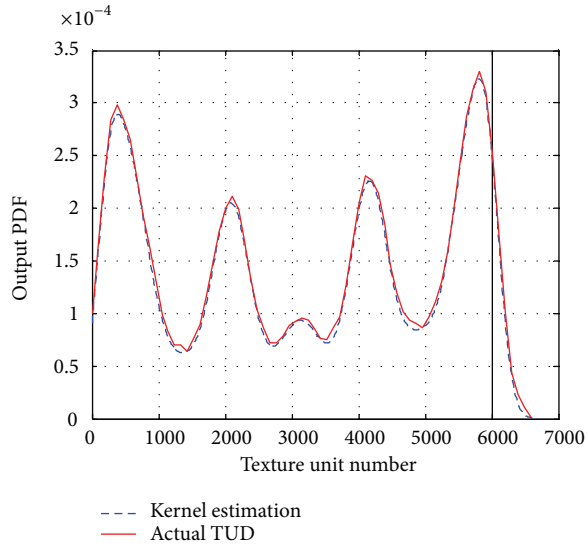

Figure 6: Normal kernel based method to approximate the actual texture unit density estimation for Figure 3.

in Figure 5. Its window width h is fixed across the entire sample. As the TUD for sulphur froth image is multipeaky and complicated, 25 kernel bases with fixed window width are used to approximate TUD, which is plotted in dashed line in Figure 5. One dotted curve presents the first and second kernel basis multiplying the corresponding weight coefficients. And the estimation result of Figure 3 froth TUD is plotted in solid line.

Figure 6 presents the kernel density estimation methods to approximate actual texture unit distribution of sulphur froth image in Figure 3. The results have shown the kernel estimation can accomplish the description of froth texture unit probability density distribution with general low feature dimensionality and high accuracy.

4. Weight PCA Model Based Performance Recognition

A fault performance is defined as the departure from an acceptable range of an observed output or operating variable. Timeous detection of fault can determine whether the abnormal condition occurs [21]. The information indicated by froth characteristics is a combining effect of multiple operational variables such as pulp level and inlet air flow in sulphur flotation. By retaining the variance of inlet air flow during a short period of time, froth texture in cleaner cell is closely related to concentrate grade which is determined by the regulation of pulp level. Human operators are in capable of performing timeous monitoring of various process variables, and the process manipulation mostly relies on heuristics of their froth view observation. Hodouin used PCA to analyze and interpret the behavior of mineral flotation and grinding circuits in a large mineral processing plant [22]. Kourti summarized the latest developments in multivariate statistical process control (MSPC) and its application for fault detection and isolation (FDI) in industrial processes [23].

4.1. Weight PCA Model. PCA is a multivariate statistical technique used in MSPC and FDI perspectives [23]. PCA uses latent variables instead of every measured variable in the process because they can better explain the behavior of the process. By monitoring the sulphur froth appearance such as froth texture, the process fault performance can be inferred and identified based on established PCA model.

The output TUD for sulphur flotation froth can be transformed to dynamic kernel weight vectors $W(t)$ through formula (8). PCA reduces the dimensionality of the original weights $W(t)$ by projecting it onto a lower dimensionality space. It obtains the principal causes of variability in the sulphur flotation process. If some of these causes change, it can be due to a fault in the process.

Consider the weight matrix $\mathbf{W} \in R^{m\times(n-1)}$, containing m samples of $n-1$ dynamic kernel weight coefficients collected under normal operation in sulphur flotation. This matrix must be normalized to zero mean and unit variance with the scale parameter vectors $\overline{w}$ and s as the mean and variance vectors, respectively. Next step to calculate PCA is to construct the covariance matrix $\mathbf{S}$:

$$\mathbf{S} = \frac{1}{n-1}\mathbf{W}^T\mathbf{W} \tag{9}$$

and performing the SVD decomposition on $\mathbf{S}$:

$$\mathbf{S} = \mathbf{V}\mathbf{\Lambda}\mathbf{V}^T, \tag{10}$$

where $\mathbf{\Lambda}$ is a diagonal matrix that contains in its diagonal eigenvalues of $\mathbf{S}$ sorted in decreasing order ($\lambda_1 \geq \lambda_2 \geq \cdots \geq \lambda_{n-1} \geq 0$). Columns of matrix $\mathbf{\Lambda}$ are the eigenvectors of $\mathbf{S}$. The transformation matrix $\mathbf{P} \in R^{m\times r}$ is generated choosing r eigenvectors or columns of $\mathbf{V}$ corresponding to r principal eigenvalues. Matrix $\mathbf{P}$ transforms the space of the measured variables into the reduced dimension space as follows:

$$\mathbf{T} = \mathbf{W}\mathbf{P}. \tag{11}$$

Columns of matrix $\mathbf{P}$ are called loadings, and elements of $\mathbf{T}$ are called scores. Scores are the values of the original measured variables that have been transformed into the reduced dimension space.

Operating in (11), the scores can be transformed into the original space as follows:

$$\widehat{\mathbf{W}} = \mathbf{T}\mathbf{P}^T. \tag{12}$$

The residual matrix $\mathbf{E}$ is calculated as

$$\mathbf{E} = \mathbf{W} - \widehat{\mathbf{W}}. \tag{13}$$

Finally the original data space can be calculated as

$$\mathbf{W} = \mathbf{T}\mathbf{P}^T + \mathbf{E} = t_1 p_1 + t_2 p_2 + \cdots + t_r p_r + \mathbf{E}. \tag{14}$$

It is very important to choose the number of principal components r, because $\mathbf{T}\mathbf{P}^T$ represents the principal sources of variability in the process, and $\mathbf{E}$ represents the variability corresponding to process noise. There is Cumulative Percent Variance (CPV) approach for determining the number of components to be retained in a PCA model as [24]. The measure of the percent variance (CPV(r) $\geq$ 95%) captured by the first r principal components is adopted as follows:

$$\mathrm{CPV}(r) = \frac{\sum_{i=1}^{r} \lambda_i}{\mathrm{trace}(\mathbf{S})}. \tag{15}$$

4.2. A New Statistical Variable Based Fault Performance Recognition. Having established a PCA model based on historical data collected when only common cause variation are present, multivariate control charts based on Hotelling's T^2 and square prediction error (SPE) or Q can be plotted. The fault performance recognition can be reduced to this two traditional variables (T^2 and Q) characterizing two orthogonal subsets of the original space. However, some of sulphur froth images contain a great deal of noise because of the acid fog in the sulphur flotation. The traditional T^2 statistic can only describe the variation in the texture information, therefore, the normal image of containing noise caused by acid fog may be detected as a fault image for its disability to handle the noise influence. As the Q statistic can represent the random noise in the froth texture, by combining T^2 statistic and Q statistic, the new statistic TQ is proposed to detect sulphur flotation fault performance more accurately:

$$TQ = \beta T^2 + (1 - \beta) Q, \tag{16}$$

where β is the regulation factor controlling the value range of TQ. β takes values between 99% and 100%.

T^2 can be calculated as the sum of squares of a new process weight vector w as follows:

$$T^2 = w^T \mathbf{P} \mathbf{\Lambda}_r^{-1} \mathbf{P}^T w, \tag{17}$$

where $\mathbf{\Lambda}_r$ is a squared matrix formed by the first r rows and columns of $\mathbf{\Lambda}$.

The sulphur flotation process is considered normal for a given significance level α if

$$T^2 \leq T_r^2 = \frac{\left(m^2 - 1\right) r}{m\,(m - r)} F_\alpha\,(r, m - r)\,, \tag{18}$$

where $F_\alpha(r, m - r)$ is the critical value of the Fisher-Snedecor distribution with m and $m - r$ degrees of freedom and α the level of significance. α takes values between 90% and 95%.

T^2 is based on the first r principal components, so that it provides a test for derivations in the latent variables that are of greatest importance to the variance of the sulphur flotation process. This statistic will only detect an event if the variation in the latent variables is greater than the variation explained by common causes.

New events can be detected by calculating the SPE or Q of the residuals of a new observation. Q statistic is calculated as the sum of squares of the residuals. The scalar value Q is a measurement of goodness of fit of the sample to the model and is directly associated with the noise as follows:

$$Q = \mathbf{e}^T \mathbf{e} \tag{19}$$

with

$$\mathbf{e} = \left(\mathbf{I} - \mathbf{P}\mathbf{P}^T\right) w. \tag{20}$$

The upper limit of this statistic can be computed as the next form:

$$Q_\alpha = \theta_1 \left[\frac{h_0 c_\alpha \sqrt{2\theta_2}}{\theta_1} + 1 + \frac{\theta_2 h_0 \left(h_0 - 1\right)}{\theta_1^2} \right]^{1/h_0} \tag{21}$$

with

$$\theta_i = \sum_{j=r+1}^{n-1} \lambda_j^i; \qquad h_0 = 1 - \frac{2\theta_1 \theta_3}{3\theta_2^2}, \tag{22}$$

where c_α is the value of the normal distribution with α, and the level of significance and λ_j are the eigenvalues of the PCA residual covariance matrix $\mathbf{E}^T\mathbf{E}/(K - 1)$.

When an unusual event occurs and it produces a change in the covariance structure of the model, it will be detected by a high value of Q.

According to the formulae (18) and (21), the critical value of the new statistical variable can be calculation as

$$TQ_\alpha = \beta T_r^2 + (1 - \beta) Q_\alpha \tag{23}$$

$$= \beta \frac{\left(m^2 - 1\right) r}{m\,(m - r)} F_\alpha\,(r, m - r) + (1 - \beta)\,\theta_1 \left[\frac{h_0 c_\alpha \sqrt{2\theta_2}}{\theta_1} + 1 + \frac{\theta_2 h_0 \left(h_0 - 1\right)}{\theta_1^2} \right]^{1/h_0}. \tag{24}$$

Through using the output TUD weight based PCA model, a criterion can be designed to detect the fault. The new statistical variable TQ is calculated on the weight PCA model. Then the critical value TQ_α of statistical variable is set as the threshold value. When the value of TQ for the new sample is larger than the threshold value TQ_α evaluated by formula (24), the fault can be detected.

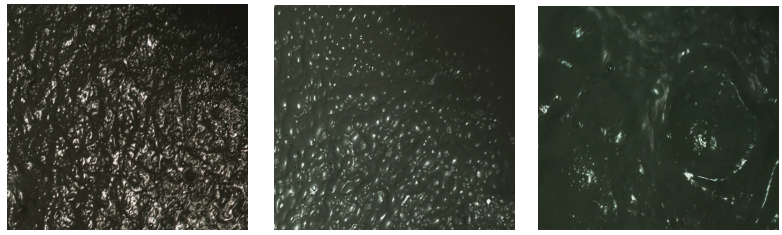

(a) (b) (c)

Figure 7: Industrial froth images captured in a continuous time: (a) normal froth image, (b) fault A froth image, and (c) fault B froth image.

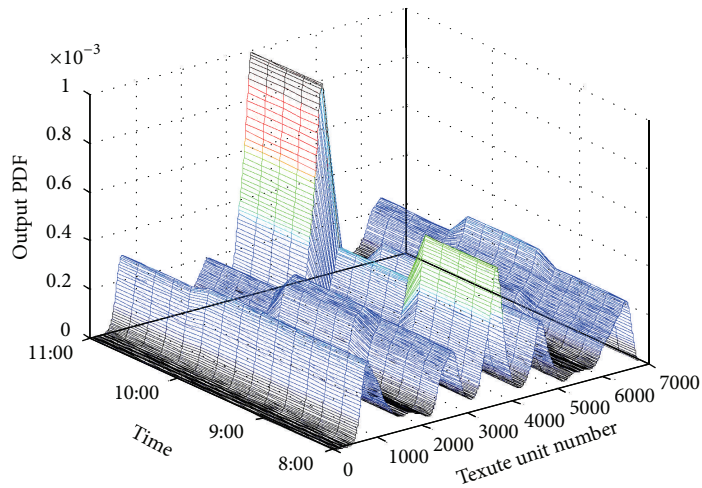

Figure 8: The 3D mesh plot of the output TUD. By applying the kernel estimation proposed in formula (8) to approximate the bubble texture unit distributions of froth images in Figure 7, the 3D mesh plot of the output TUD when fault occurs is presented.

5. Application Results and Discussion

To evaluate the proposed weight PCA model based fault detection approach, a series of industrial experiments are carried out in a Chinese sulphur froth flotation plant. In the test runs, froth image videos are captured through the previously introduced monitoring system in the last cleaner flotation cell. Subsequently, the froth videos are processed by the developed image analysis software which is capable of extracting froth features such as TUD online. Figure 7 presents the three types of froth images in different performance, which are collected and analyzed under the same condition in terms of resolution, angle, light condition, position, view scale, and so forth.

In practical sulphur flotation process experiments, the air flow rate and feed-in conditions are kept at a steady state so as to stabilize the production process. The adjustment of pulp level (or froth depth) becomes the major manipulating parameter, which directly determines flotation performance. As an indication of flotation performance, the froth texture feature is one of determinants of mineral separation efficiency. Bubbles with relative complex texture generally carry more valuable mineral particles, whose corresponding pulp level value is to be maintained to an acceptable bounded range. When one of the dominant operating variable pulp level is fluctuated, in this case the regulation of slurry underflow, froth surface visual features such as froth texture and color spectral information are reacting to the change of pulp level value. An increase in pulp level was considered, such that its simultaneous effect on froth texture unit distribution can be identified. As is shown in Figure 7, the froth images evolved as pulp level value varied gradually during a period, and the corresponding operational conditions were measured at the same time.

As for texture unit number calculation, normal kernel with following basis functions is selected according to formula (5). The window width h is set to be 200 as a smoothing parameter, and centered points of each kernel $X_i = 250 * i$, $(i = 1, \ldots, 25)$. Since the froth texture unit involved ranges from 0 to 6560, the kernel functions with fixed window width are supposed to cover the entire texture unit value range. Thus, the froth TUD can be approximated by (8), where $n = 25$. The weights $W(t)$ of normal kernel expansion have dimension of 25, and only 24 of which are independent.

By applying the kernel estimation on the TUDs of froth images in Figure 7, the 3D mesh plot of the output TUD is shown in Figure 8. At an hourly interval, the froth image video is captured at the point since it is reasonable to consider that the froth TUD is representative during a short-time period in this study case. Meanwhile, the process operational conditions are measured correspondingly. As can be seen, the froth TUD tends to shift dramatically with occurring a low peak when the slurry underflow increased at 9:00,

Table 1: The detection performance of the testing database.

	Samples with correct detection	Samples with incorrect detection	Accuracy rate (%)
Normal status	134	6	95.71
Fault A status	48	5	90.57
Fault B status	46	4	92
Total	228	15	93.83

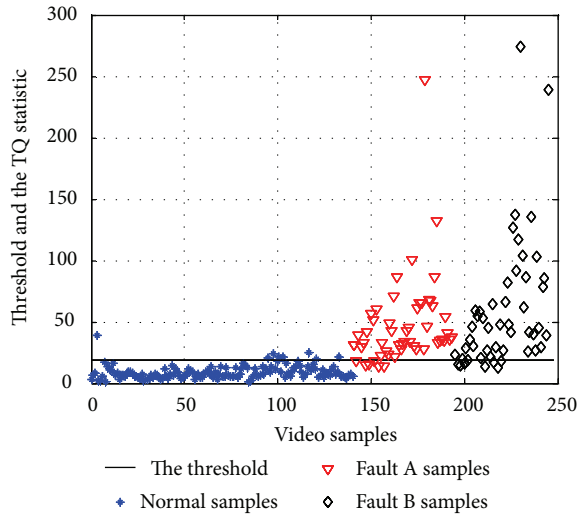

Figure 9: The TQ statistics of the testing froth video database.

which resulted in froth depth value increased from 190 mm to 350 mm in response. Then the excessive decrease of froth depth to 30 mm produces a corresponding upward change of the peak of TUD curve. Accordingly, the separation performance mineral grade deteriorated from 81% at 8:00 to 50% at 11:00.

The weight PCA model applied in this case is established as

$$\mathbf{W}_T = t_1 p_1 + t_2 p_2 + \cdots + t_r p_r + \mathbf{E}, \tag{25}$$

where $r = 9$.

According to the formula (24), threshold value can be calculated as $TQ_a = 18.11$ by setting $\alpha = 0.95$, $\beta = 0.99$. Setting Figure 7(a) as the normal TUD, Figure 9 shows the threshold with solid line and the TQ statistics for froth images in Figure 7. As can be seen, Figures 7(b)-7(c) are clearly identified as fault status because the statistic $TQ > TQ_a$, which are consistent with the observation results from human operators.

Attempts have been made in calculating false alarm rate on a testing database. The testing data consist of 243 offline froth videos captured from the sulphur flotation industry during August of 2011. The fault detection is accomplished by a threshold criterion calculated from formula (24), according to which the TQ statistic above the threshold value indicates that a fault occurs. Table 1 gives the detection performance of the testing database. As can be seen in Figure 9, solid line represents the threshold for fault detection, and asterisks are TQ statistics of each normal video sample. Triangles and diamonds are the samples with fault A and fault B. The total fault detection accuracy on the database is 93.83%. It is possible that the false detection alarm ascribes to the texture unit number calculation malfunction of the captured froth images.

6. Conclusion

In this paper the description of texture unit number probability density distribution and its relationship to pulp level operational status are investigated. Unlike traditional discussion of froth texture feature focusing mostly on second-order statistics based on GLCM including angular second moment, entropy, moment of inertia, and moments of deficit and relevance, a nonparametric estimation method is proposed to describe the TUD more accurately based on the fixed normal kernel basis, and the fault performance is detected through the proposed TQ statistic. Desired fault detection for pulp level regulation in froth flotation industry is achieved using the proposed method.

Acknowledgments

This work was financially supported by Key Program of Natural Science Foundation of China under Grant no. 61134006, National Science and Technology Pillar Program of China under Grant no. 2012BAF03B05, and National Science Fund for Distinguished Young Scholars of China under Grant no. 61025015.

References

[1] C. Citir, Z. Aktas, and R. Berber, "Off-line image analysis for froth flotation of coal," *Computers and Chemical Engineering*, vol. 28, no. 5, pp. 625–632, 2004.

[2] W. Wang, F. Bergholm, and B. Yang, "Froth delineation based on image classification," *Minerals Engineering*, vol. 16, no. 3, pp. 1183–1192, 2003.

[3] C. Aldrich, C. Marais, B. J. Shean, and J. J. Cilliers, "Online monitoring and control of froth flotation systems with machine vision: a review," *International Journal of Mineral Processing*, vol. 96, no. 1–4, pp. 1–13, 2010.

[4] V. Hasu, J. Hätönen, and H. Hyötyniemi, "Analysis of flotation froth appearance by design of experiment," in *Proceedings of the IFAC Workshop on Future trends in Automation in Mineral and Metal*, pp. 22–24, Espoo, Finland, 2000.

[5] G. Bonifazi, S. Serranti, F. Volpe, and R. Zuco, "Characteristisation of flotation froth colour and structure by machine vision," *Computers and Geosciences*, vol. 27, no. 9, pp. 1111–1117, 2001.

[6] P. N. Holtham and K. K. Nguyen, "On-line analysis of froth surface in coal and mineral flotation using JKFrothCam," *International Journal of Mineral Processing*, vol. 64, no. 2-3, pp. 163–180, 2002.

[7] D. W. Moolman, C. Aldrich, and J. S. J. Van Deventer, "The monitoring of froth surfaces on industrial flotation plants using connectionist image processing techniques," *Minerals Engineering*, vol. 8, no. 1-2, pp. 23–30, 1995.

[8] J. Kaartinen, J. Hätönen, H. Hyötyniemi, and J. Miettunen, "Machine-vision-based control of zinc flotation-A case study," *Control Engineering Practice*, vol. 14, no. 12, pp. 1455–1466, 2006.

[9] B. J. Shean and J. J. Cilliers, "A review of froth flotation control," *International Journal of Mineral Processing*, vol. 100, no. 3-4, pp. 57–71, 2011.

[10] J. J. Liu and J. F. MacGregor, "Froth-based modeling and control of flotation processes," *Minerals Engineering*, vol. 21, no. 9, pp. 642–651, 2008.

[11] J. M. Hargrave and S. T. Hall, "Diagnosis of concentrate grade and mass flowrate in tin flotation from colour and surface texture analysis," *Minerals Engineering*, vol. 10, no. 6, pp. 613–621, 1997.

[12] N. Saghatoleslam, H. Karimi, R. Rahimi, and H. H. A. Shirazi, "Modeling of texture and color froth characteristics for evaluation of flotation performance in sarcheshmeh copper pilot plant using image analysis and neural networks," *International Journal of Engineering B*, vol. 17, no. 2, pp. 121–130, 2004.

[13] G. Bartolacci, P. Pelletier, J. Tessier, C. Duchesne, P. A. Bossé, and J. Fournier, "Application of numerical image analysis to process diagnosis and physical parameter measurement in mineral processes-Part I: flotation control based on froth textural characteristics," *Minerals Engineering*, vol. 19, no. 6–8, pp. 734–747, 2006.

[14] D. C. He and L. Wang, "Texture unit, texture spectrum, and texture analysis," *IEEE Transactions on Geoscience and Remote Sensing*, vol. 28, no. 4, pp. 509–512, 1990.

[15] J. X. Li and L. T. Tran, "Nonparametric estimation of conditional expectation," *Journal of Statistical Planning and Inference*, vol. 139, no. 2, pp. 164–175, 2009.

[16] L. Guo, H. Wang, and A. P. Wang, "Optimal probability density function control for NARMAX stochastic systems," *Automatica*, vol. 44, no. 7, pp. 1904–1911, 2008.

[17] P. Jampana, S. L. Shah, and R. Kadali, "Computer vision based interface level control in separation cells," *Control Engineering Practice*, vol. 18, no. 4, pp. 349–357, 2010.

[18] D. Beneventi, X. Rousset, and E. Zeno, "Modelling transport phenomena in a flotation de-inking column: focus on gas flow, pulp and froth retention time," *International Journal of Mineral Processing*, vol. 80, no. 1, pp. 43–57, 2006.

[19] J. J. Cilliers and C. L. E. Swartz, "Simulation of quantitative fault diagnosis in backfill hydrocyclones," *Minerals Engineering*, vol. 8, no. 8, pp. 871–882, 1995.

[20] C. H. Xu, W. H. Gui, C. H. Yang, H. Q. Zhu, Y. Q. Lin, and C. Shi, "Flotation process fault detection using output PDF of bubble size distribution," *Minerals Engineering*, vol. 26, no. 1, pp. 5–12, 2012.

[21] T. Kourti, "Process analysis and abnormal situation detection: from theory to practice," *IEEE Control Systems Magazine*, vol. 22, no. 5, pp. 10–25, 2002.

[22] D. Hodouin, J. F. MacGregor, M. Hou, and M. Franklin, "Multivariate statistical analysis of mineral processing plant data," *CIM Bulletin of Mmerul Processing*, vol. 86, no. 975, pp. 23–34, 1993.

[23] T. Kourti, "Application of latent variable methods to process control and multivariate statistical process control in industry," *International Journal of Adaptive Control and Signal Processing*, vol. 19, no. 4, pp. 213–246, 2005.

[24] D. Garcia-Alvarez, M. J. Fuente, and G. I. Sainz, "Fault detection and isolation in transient states using principal component analysis," *Journal of Process Control*, vol. 22, no. 3, pp. 551–563, 2012.